



Original Article

Thermal stability and hydration behavior of ritonavir sulfate: A vibrational spectroscopic approach [☆]Kaweri Gambhir ¹, Parul Singh ¹, Deepak K. Jangir, Ranjana Mehrotra ^{*}

Quantum Optics and Photon Physics, CSIR-National Physical Laboratory, Dr. K.S. Krishnan Marg, New Delhi 110012, India

ARTICLE INFO

Article history:

Received 13 December 2014

Received in revised form

25 April 2015

Accepted 5 May 2015

Available online 23 May 2015

Keywords:

Ritonavir sulfate

Diffuse reflectance infrared Fourier transform spectroscopy

Raman spectroscopy

Thermal degradation

Hydration

ABSTRACT

Ritonavir sulfate is a protease inhibitor widely used in the treatment of acquired immunodeficiency syndrome. In order to elucidate the inherent stability and sensitivity characteristics of ritonavir sulfate, it was investigated under forced thermal and hydration stress conditions as recommended by the International Conference on Harmonization guidelines. In addition, competency of vibrational (infrared and Raman) spectroscopy was assessed to identify structural changes of the drug symbolizing its stress degradation. High performance liquid chromatography was used as a confirmatory technique for both thermal and hydration stress study, while thermogravimetric analysis/differential thermal analysis and atomic force microscopy substantiated the implementation of vibrational spectroscopy in this framework. The results exhibited high thermal stability of the drug as significant variations were observed in the diffuse reflectance infrared Fourier transform spectra only after the drug exposure to thermal radiations at 100 °C. Hydration behavior of ritonavir sulfate was evaluated using Raman spectroscopy and the value of critical relative humidity was found to be > 67%. An important aspect of this study was to utilize vibrational spectroscopic technique to address stability issues of pharmacological molecules, not only for their processing in pharmaceutical industry, but also for predicting their shelf lives and suitable storage conditions.

© 2015 Xi'an Jiaotong University. Production and hosting by Elsevier B.V.

Open access under [CC BY-NC-ND license](https://creativecommons.org/licenses/by-nc-nd/4.0/).

1. Introduction

Inhibition of human immunodeficiency virus (HIV) protease has been recognized as an important approach for therapeutic intervention of acquired immunodeficiency syndrome (AIDS) [1]. Protease inhibitors are the drugs which play an instrumental role in the reduction of morbidity and mortality among people with HIV infection [2,3]. Amongst the family of protease inhibitors, ritonavir sulfate has revolutionized HIV therapy due to its selective, competitive and reversible inhibitory effects on both HIV-1 and HIV-2 proteases [4]. Ritonavir, {[5S-(5R*,8R*,10R*,11R*)]-10-hydroxy-2-methyl-5-(1-methylethyl)-1-[2-(1-methylethyl)-4-thiazolyl]-3,6-dioxo-8,11-bis(phenylmethyl)-2,4,7,12-tetraazatridecan-13-oic acid, 5-thiazolylmethyl ester} (Fig. 1), is a synthetic organic compound derived from N-carbamoyl-alpha amino acids and their derivatives.

The stability of pharmaceutical molecules is a matter of great concern as it affects the safety and efficacy of the drug product. Therefore, the International Conference on Harmonization (ICH) Q1A guideline entitled "Stability testing of new drug substances

and products" requires stress testing to be carried out in order to elucidate the inherent stability and sensitivity characteristics of the active substance [5]. However, literature supports limited analytical methods established for the stability studies of the solid dosage form of ritonavir sulfate. While high performance thin layer chromatography (HPTLC) has been used for simultaneous determination of ritonavir and lopinavir in capsules [6]. A few liquid chromatography–mass spectroscopy (LC–MS) methods have been reported for analysis of ritonavir and its metabolites in biological fluids [7–10]. International Pharmacopoeia (Ph. Int.) describes a liquid chromatography method to separate ritonavir and its impurities [4]. Determination of ritonavir in bulk dosage form using spectrophotometric and potentiometric methods has also been described [11–15]. In recent years, several high performance liquid chromatography (HPLC) methods for simultaneous determination of antiretroviral drugs in plasma have been demonstrated [16,17]. Nevertheless, HPLC has been widely used for the stress degradation study of pharmaceuticals, it has some disadvantages in terms of cost performance, time consumption and necessary equipment, such as the use of expensive disposable cartridges at solid-phase drug extraction, gradient elution control by a gradient HPLC pump system and the ultraviolet detection at multiple wavelengths. Therefore, in the present scenario, a simplified technique is desirable for addressing these issues.

[☆]Peer review under responsibility of Xi'an Jiaotong University.^{*} Corresponding author. Fax: +91 11 45609310.E-mail address: ranjana@nplindia.org (R. Mehrotra).¹ Equal contribution.

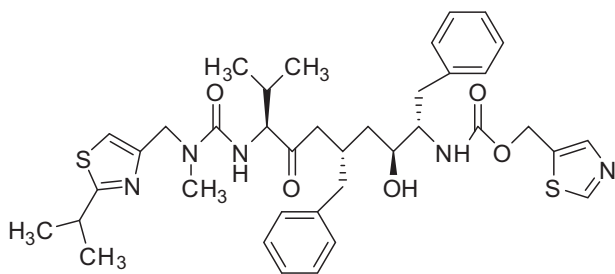


Fig. 1. Chemical structure of ritonavir sulfate.

Vibrational spectroscopy has an edge over the above mentioned techniques for studying pharmaceutical systems at molecular level as it is a nondestructive and noninvasive technique, and is sensitive to structural conformational aspects and the environment of the compound to be analyzed [18]. It also offers substantial advantages in terms of speed, lends them to in-process monitoring of the structure and does not require hazardous organic solvents. Vibrational spectroscopy has been employed by various researchers to evaluate the photo-stability of drugs. The photo-stability of nifedipine and corresponding transformations during the shelf-life of the solid dosage form of a drug has been determined using Fourier transform infrared (FTIR) spectroscopy [19]. Similarly, the photo-stability of carbamazepine polymorphs and nifedipine has been studied using Fourier transform reflection-absorption spectroscopy [20,21]. In our previous study, we applied diffuse reflectance infrared spectroscopy to evaluate the stability of some antiretroviral and anticancer drugs [22–24]. Raman spectroscopy has been successfully used for the quantitative analysis of polymorphic mixture of carbamazepine [25]. Sardo et al. [26] used Raman spectroscopy to monitor reversible-hydration kinetic processes of niclosamide. Moreover, hydration and dehydration characteristics of theophylline have been monitored using Raman spectroscopy [27].

The present study was conducted to assess the feasibility of vibrational spectroscopy to address thermal as well as hydration stability issues of ritonavir sulfate. The critical temperature and critical relative humidity (RH) of ritonavir sulfate estimated through this work are necessary not only for its processing in pharmaceutical industry but also for predicting its shelf life and suitable storage conditions. In this framework, diffuse reflectance infrared Fourier transform (DRIFT) spectroscopy was used to evaluate the thermal stability of the drug. HPLC and thermogravimetric analysis (TGA)/differential thermal analysis (DTA) were used to substantiate the inferences drawn from the spectroscopic analysis of the thermally degraded drug. Furthermore, Raman spectroscopy, a water transparent technique, was used to study the hydration stress behavior of ritonavir, and HPLC was also used as a confirmatory technique for hydration stress behavior. Moreover, atomic force microscopy (AFM) analysis was carried out to depict changes in the topographical morphology of the hydrated form of ritonavir sulfate.

2. Experimental

2.1. Materials and methods

Tablets of ritonavir sulfate used in this investigation were procured from Cipla Pharmaceuticals Limited, India. Spectroscopic grade potassium bromide (KBr) was bought from BDH Laboratory Suppliers, England. Methanol (CH₄O), potassium phosphate (KH₂PO₄), acetonitrile (C₂H₃N) and 0.05 M phosphoric acid (H₃PO₄) used in the study were of HPLC grade and obtained from Qualigens Fine

Chemicals. Millipore purified water (resistance ~18.2 MΩ) from Scholar-UV Nex UP 1000 system was used for HPLC analysis. All other reagents were of analytical grade and used without further purification.

2.2. Thermal degradation studies

2.2.1. Sample preparation

Ritonavir sulfate was thermally degraded using Linkam TP 92, HFS 91/Hot stage plate with platinum resistor. The setup included a small aluminum dish in which the drug powder was kept on the silver block in the hot stage. The drug samples for the study were heated at different temperatures ranging from 30 to 120 °C with an increment of 10 °C for a period of 1–6 h with an increment of 1 h at each temperature. Besides this, a fresh drug sample was used at each temperature and retention time. Then, the thermally treated samples were cooled down to room temperature before being subjected to DRIFT measurements. The heating and cooling rate of the hot stage was maintained at 10 °C/min.

2.2.2. DRIFT spectroscopic measurements

To characterize thermally treated ritonavir sulfate samples, homogenous sample mixtures were prepared by dispersing 5% (m/m) of thermally treated drug powder in spectroscopic grade potassium bromide. The sample mixtures were then kept in the sample holder of Varian 660 Fourier transform infrared spectrophotometer equipped with Pike Technologies, diffuse reflectance accessory operating with a Global source, in combination with a KBr beam splitter and deuterated triglycine sulfate (DTGS) detector. The infrared spectra of the drug powder before and after exposure to thermal radiation were recorded in the scan range of 400–4000 cm⁻¹ with a resolution of 4 cm⁻¹. A total of 256 scans were collected for each spectrum. Background spectrum was also recorded with ground potassium bromide powder under the same experimental conditions before collecting each sample scan.

2.2.3. HPLC measurements

HPLC analysis of thermally degraded ritonavir sulfate was performed on a Shimadzu HPLC (UFLC, Prominence) equipped with an LC-20AD binary pump, an SPD-20A variable wavelength UV-vis detector, a CTO-20A column oven, degasser and a manual injector fitted with 20 μL sample loop. The instrument was controlled by LC software. A Phenomenex C₁₈ column (250 mm × 4.6 mm, 5 μm) was used for analysis. The mobile phase consisting of acetonitrile: 0.05 M phosphoric acid (55:45, v/v), was ultrasonicated and vacuum filtered by passing through a 0.44 μm pore size membrane filter prior to use. The standard stock solutions of fresh ritonavir sulfate at a concentration of 1.0 mg/mL, after exposure to thermal radiations and different RH treated samples, were prepared in the mobile phase. The prepared solution was ultrasonicated for 20 min, vacuum filtered through a 0.44 μm membrane filter and then a 0.22 μm membrane filter before being fed to the manual injector. The flow rate was adjusted to 1.0 mL/min and the injection volume of 20 μL was maintained. All the chromatograms were recorded at a wavelength of 210 nm with the column temperature maintained at 40 °C.

2.2.4. TGA/DTA studies

For comprehensive analysis of ritonavir sulfate's thermal behavior, TGA/DTA measurements of the drug were conducted on a Shimadzu TA 60 thermal analyzer with 10 mg of sample under a nitrogen flow of 40 mL/min with a heating rate of 10 °C/min from 35 to 350 °C. The experiment was performed in triplicate to check the reproducibility.

2.3. Hydration studies

2.3.1. Sample preparation

Approximately 0.5 g of the anhydrous ritonavir sulfate samples were transferred to glass petridishes and exposed to different RH conditions which were obtained using various saturated salt solutions. The RH values taken from literature [28] were manually optimized and were as follows: 9% (KOH), 13% (LiCl), 20% ($\text{KC}_2\text{H}_3\text{O}_2$), 28% (KF), 30% (CaCl_2), 42% [$\text{Zn}(\text{NO}_3)_2$], 48% (KSCN), 66% (NaNO_2), 73% (KHSO_4), 81% [$(\text{NH}_4)_2\text{SO}_4$], 82% (NH_4Cl), 86% (Na_2SO_3), 92% (KNO_3). Similarly, 0% and 100% RH were achieved using silica and millipore water, respectively. To equilibrate the humidity conditions, each sample was exposed to different relative humidity for one week. All the experiments were performed at ambient temperature and repeated three times to check its reproducibility.

2.3.2. FT-Raman measurements

The hydration behavior of ritonavir sulfate treated under various RH conditions, was investigated using Perkin Elmer FT-Raman spectrophotometer equipped with Nd:YAG laser with an excitation wavelength of 1064 nm. The laser power was set to 500 mW. A total of 256 scans were accumulated for each spectrum with a resolution of 4 cm^{-1} .

2.3.3. AFM measurements

For AFM measurements, discs of ritonavir sulfate samples, after exposure to different RH environments, were prepared by placing approximately 200 mg of the sample in a press dye at a pressure of 10 t for 5 min. Raman spectroscopy of the discs did not depict any change in the spectra as a consequence of the applied pressure. AFM measurements of the discs were performed using Witec AFM-micro-Raman instrument. All measurements were acquired in air using tapping mode with silicon cantilevers with a nominal force constant and resonance frequency of approximately 50 N/m and 300 kHz, respectively.

3. Results and discussion

3.1. Thermal degradation analysis

3.1.1. DRIFT spectroscopic analysis

Ritonavir sulfate was thermally treated at temperatures ranging from 30 to $120\text{ }^\circ\text{C}$ beyond which the physical state of the drug started changing. The DRIFT spectrum of the thermally untreated drug in the frequency range of $4000\text{--}400\text{ cm}^{-1}$ is shown in Fig. 2. The characteristic spectrum of fresh ritonavir sulfate showed sharp peaks at 3085 and 3285 cm^{-1} corresponding to C=C–H

asymmetric stretching vibrations of benzene ring and to N–H stretching vibrations of amide groups, respectively, while those peaks at 2953, 2918 and 2853 cm^{-1} are due to C–H symmetric and antisymmetric stretching vibrations of alkanes [29]. The absorption band owing to the carbonyl group of ester linkage was observed at 1725 cm^{-1} [30]. In addition, 1678 cm^{-1} band corresponds to C=O stretching vibrations of amide group. Similarly, bands at 1524 and 1496 cm^{-1} can be assigned to C=C stretching vibration of aromatic carbons presenting in the benzene ring, while infrared band at 1461 cm^{-1} is due to C–H₃ bending vibrations [29]. Furthermore, the absorption band at 1372 cm^{-1} is attributed to C–H rocking vibration of alkanes. C–O stretching vibrations of esters were found in the infrared region 1000 to 1300 cm^{-1} [29]. Besides this, the band at 936 cm^{-1} corresponds to O–H bending vibrations of carboxylic acid. In the frequency range of $400\text{--}900\text{ cm}^{-1}$, out of plane C–H distortions were visible amongst which the band at 739 cm^{-1} may be due to the presence of C–H bending vibrations depicting aromatic substitution [31].

The overlaid DRIFT spectra of ritonavir sulfate collected after exposure to thermal radiations at different temperatures are shown in Fig. 3 and significant changes at higher temperatures in frequency region of $1800\text{--}400\text{ cm}^{-1}$ are illustrated in Fig. 4. No major structural changes in terms of infrared band position or intensity were noticed up to $70\text{ }^\circ\text{C}$, although trivial intensity variations in the region of –OH stretching ($3000\text{--}4000\text{ cm}^{-1}$) were observed, which may be attributed to loss of water adsorbed. Considerable intensity variation was observed in the spectra at $80\text{ }^\circ\text{C}$, which revealed that the drug started degrading around this temperature. Significant changes were detected in the spectra after exposure at $100\text{ }^\circ\text{C}$ for 5 h. The intensity of characteristic peaks ascribed to ritonavir sulfate started diminishing at the above mentioned temperature. The higher frequency region attributed to CH/NH/OH stretching was relatively stable, except for slight intensity variation observed. The intensity of bands at 2953, 2918 and 2853 cm^{-1} which were due to H–C–H symmetric and antisymmetric stretching vibrations of alkanes diminished. The infrared absorption band at 1725 cm^{-1} owing to the carbonyl group of ester linkage also vanished. Slight intensity variation was observed in the band at 936 cm^{-1} which corresponds to O–H bending vibrations of carboxylic acid. Besides this, a drop in the intensity was observed at 1372 and 1239 cm^{-1} bands which correspond to C–H rocking vibration of alkanes and C–O stretching vibrations of esters, respectively. Similarly, bands at 1117, 1025 and 703 cm^{-1} disappeared whereas a new peak at 444 cm^{-1} originated in the spectra of degraded drug (inset of Fig. 4). This band may be tentatively assigned to out of plane C–H distortion due to thiazole moiety [32]. It can be used as a marker band for the degradation of ritonavir sulfate. Similarly, peaks at 1286 and 845 cm^{-1} owing to

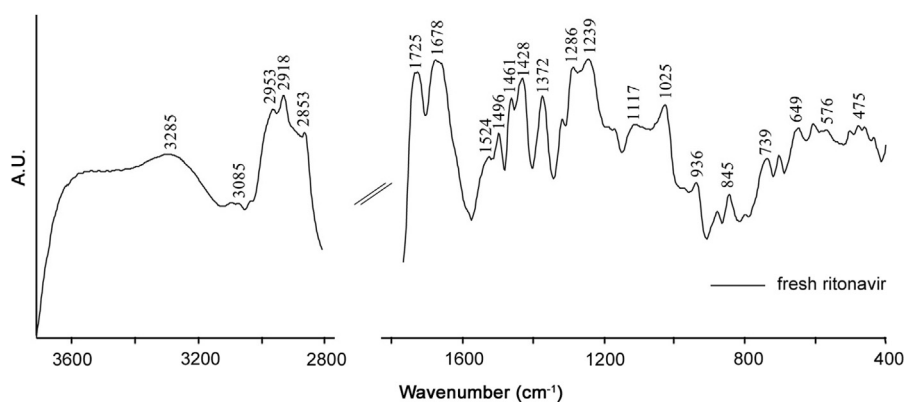


Fig. 2. DRIFT spectrum of ritonavir sulfate in the frequency range of $4000\text{--}400\text{ cm}^{-1}$.

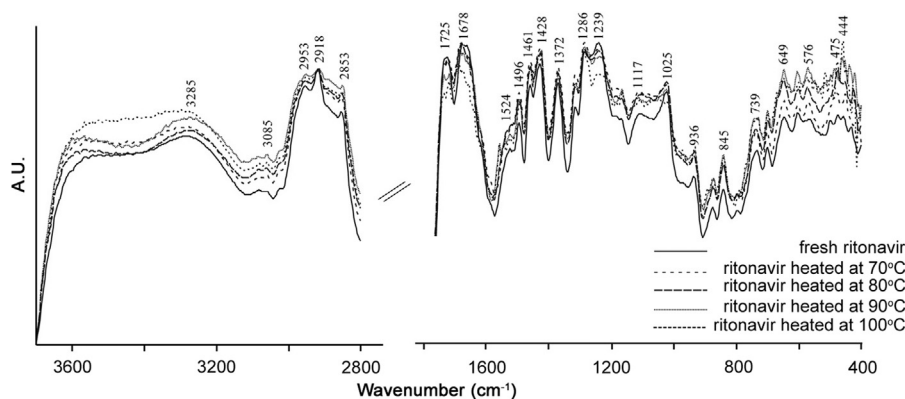


Fig. 3. Overlaid DRIFT spectra of ritonavir sulfate in the frequency range of 4000–400 cm^{-1} .

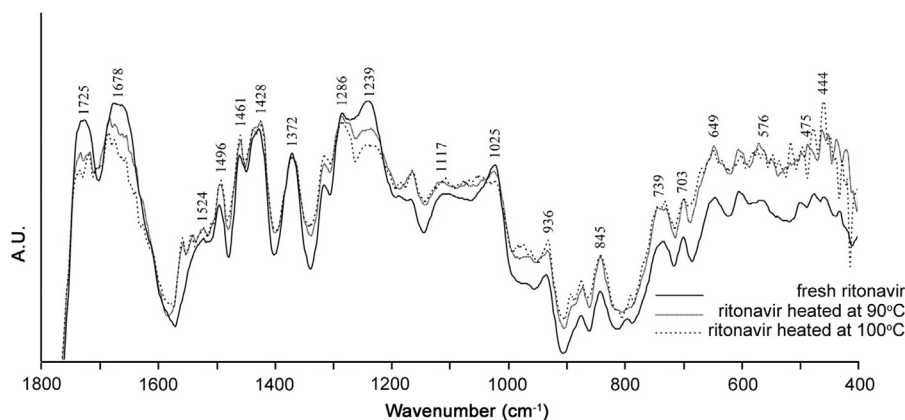


Fig. 4. Overlaid DRIFT spectra of ritonavir sulfate at higher temperatures in the region of 1800–400 cm^{-1} .

Table 1

Changes in DRIFT frequencies after ritonavir sulfate exposure to higher temperatures and their proposed assignments

Frequency (cm^{-1})	Vibrational assignments	Remarks
2953	H–C–H symmetric and antisymmetric stretch of alkanes	Peaks became less intense at higher temperature.
2918	H–C–H symmetric and antisymmetric stretch of alkanes	Intensity of peak decreased.
2853	H–C–H symmetric and antisymmetric stretch of alkanes	Peaks became less intense at higher temperature.
1725	C=O carbonyl group of ester linkage	The peak vanished.
1372	C–H rock of alkanes	Intensity of peak decreased.
1286	C–O stretch of esters	The peak became more intense.
1239	C–O stretch of esters	Peaks become less intense at higher temperature.
1117	C–O stretch of esters	The peak disappeared at higher temperature.
1025	C–O stretch of esters	The peak disappeared.
845	out of plane C–H distortions	The peak became more intense.
703	out of plane C–H distortions	The peak disappeared.

C–O stretching vibrations of esters and C–H “oop” modes showed more intense behavior on degradation. The variations in the band positions and intensity observed in the infrared spectra of the drug when exposed to intense thermal radiations are listed in Table 1.

The results of DRIFT spectroscopy presented here showed that major structural changes took place in ritonavir sulfate after exposure to thermal radiation at 100 °C, whereas it got completely decomposed after 200 °C. Further, these results indicated higher thermal stability of the drug as illustrated by TGA/DTA outcomes.

3.1.2. HPLC analysis

HPLC chromatogram of unexposed ritonavir sulfate as shown in Fig. 5A revealed that the drug was separated at a retention time of about 6 min. Further, the chromatographic results of thermally exposed ritonavir remained the same in terms of peak intensity

and retention time up to 80 °C, beyond which an additional peak was observed marking onset of the drug degradation process. And an additional peak along with a decrease in the characteristic peak intensity of ritonavir sulfate was observed at 100 °C (exposure time 5 h) and remained consistent up to 120 °C. Thus, it can be inferred that maximum degradation was attained at 100 °C, and HPLC results substantiated DRIFT outcomes. The comparative chromatogram of thermally exposed (100 °C, 5 h) drug with that of unexposed drug is shown in Fig. 5B.

3.1.3. TGA/DTA

Ritonavir sulfate was analyzed using TGA/DTA to get an idea about the thermal decomposition behavior of the drug. In TGA, the change in sample mass was measured by a thermobalance as a function of temperature. Fig. 6 shows the TGA curve of ritonavir

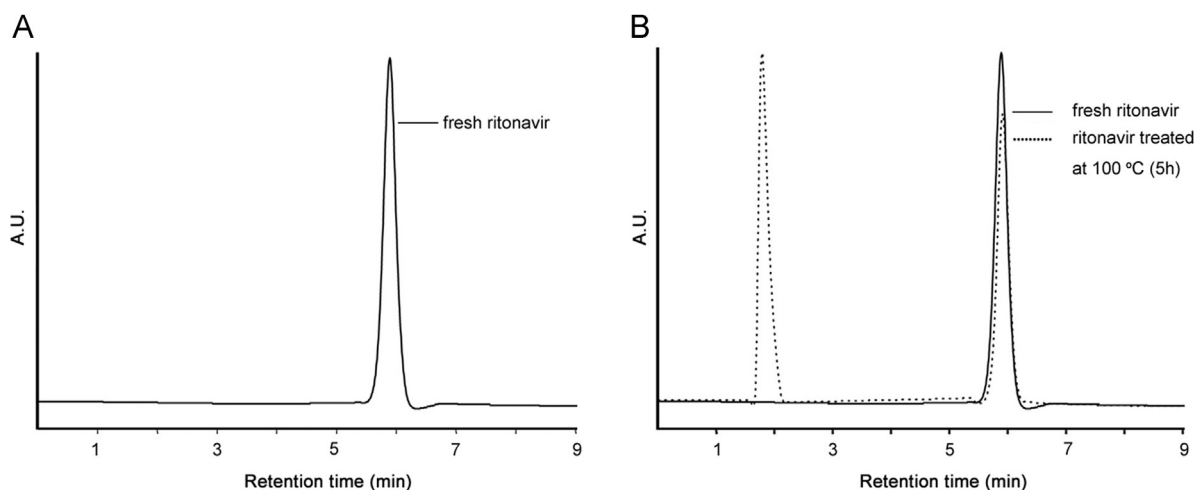


Fig. 5. (A) HPLC chromatogram of unexposed ritonavir sulfate and (B) overlaid chromatogram of unexposed and thermally degraded drug at 100 °C at exposure time of 5 h.

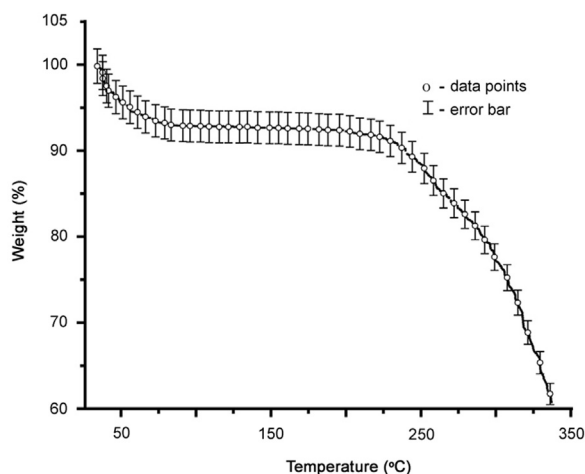


Fig. 6. TGA curve of ritonavir sulfate.

sulfate. High thermal stability of the drug can be evident from the thermal curve as the decomposition started at about 200 °C. The major weight loss occurred between 220 and 300 °C. DTA curve was in accordance with TGA results.

3.2. Hydration studies

3.2.1. Raman analysis

Raman spectrum of anhydrous ritonavir sulfate is shown in Fig. 7. The band at 1732 cm^{-1} was attributed to the NH...O stretching. The Raman frequency at 1665 cm^{-1} is assigned to the NH...N stretching vibration. The band at 1602 cm^{-1} corresponds to the amide CO stretching vibration. N=N stretching was observed at about 1492 cm^{-1} [33]. The absorption band at 1230 cm^{-1} is assigned to the C=O stretching vibration. The ring stretching was observed at 1205 cm^{-1} . O–HN deformation was observed at 1115 cm^{-1} . The Raman frequency at 932 cm^{-1} may be attributed to symmetric C–O–C stretching. In-plane ring bending vibration was observed at 750 cm^{-1} [33].

Fig. 8 compares the Raman spectra of untreated ritonavir sulfate with those of collected ones after the drug exposure to RH (82%). Remarkable differences in terms of band intensity were visible in the overlaid spectra, which may be associated with the structural changes induced by hydration. The tentative assignments of the bands where differences occurred are presented in Table 2.

It can be seen that NH...O stretching vibration that appeared at 1732 cm^{-1} in anhydrous form disappears on hydration. The band at 1665 cm^{-1} that is assigned to NH...N stretching became less intense and shifted towards lower wavenumber on hydration. N=N

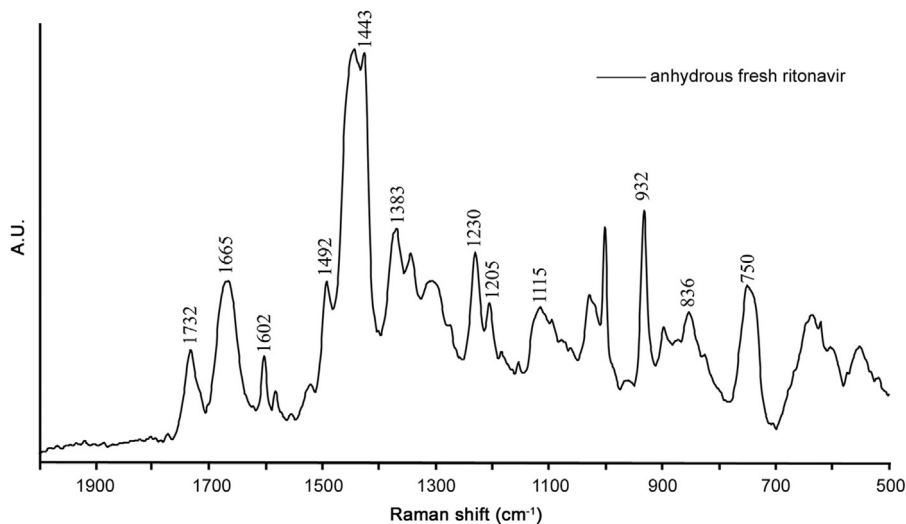


Fig. 7. Raman spectra of ritonavir sulfate in the region of 1800–600 cm^{-1} .

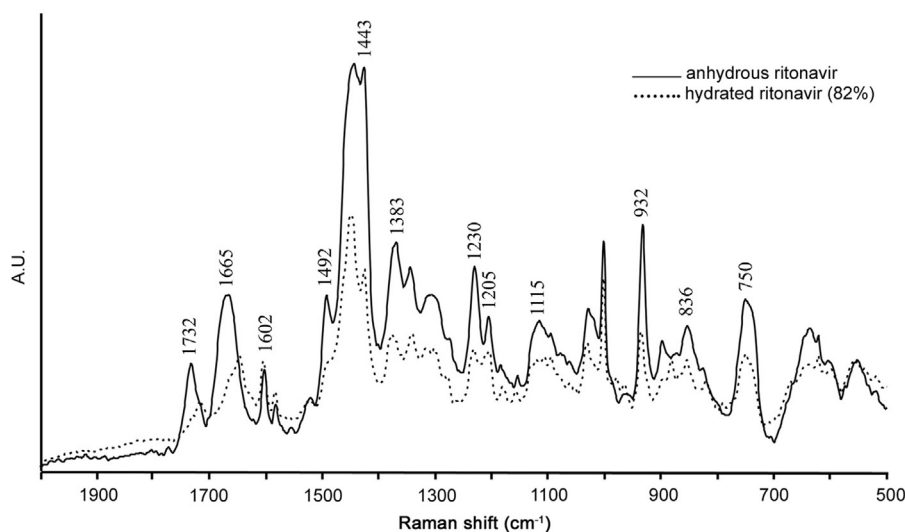


Fig. 8. Overlaid Raman spectra of ritonavir sulfate after exposure to high relative humidity.

Table 2

Changes in Raman frequencies after exposing ritonavir sulfate to higher relative humidity and their proposed assignments

Frequency (cm^{-1})	Vibrational assignments	Remarks
1732	NH...O stretching	The band disappeared at higher humidity.
1665	NH...N stretching	Intensity of peak decreased and shifted towards lower wavenumber.
1602	CO amide	–
1492	N=N stretching	The band disappeared at higher humidity.
1443	O–H stretching	The peak became sharp at higher humidity. It may be due to hydrate formation.
1230	C=O stretching	Intensity of peak decreased.
1205	Ring stretching	The peak disappeared.
1115	O...NH deformation	–
932	Symmetric C–O–C stretch	Intensity of peak decreased.
750	In plane ring bending	Peak became less intense at higher humidity.

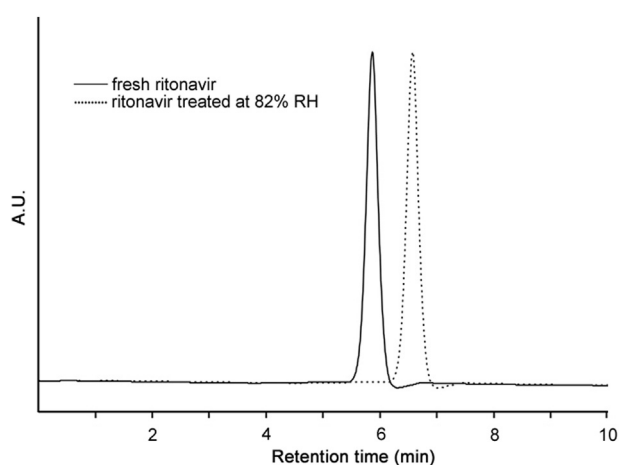


Fig. 9. Overlaid HPLC chromatogram of unexposed and hydrated (82% RH) drugs.

stretching band at 1492 cm^{-1} disappeared after the drug exposure to higher humidity. O–H stretching peak observed at 1443 cm^{-1} in anhydrous form became sharp at higher humidity. This may be due to the hydrogen bonding on hydrate formation. The intensity of C=O stretching vibration at 1230 cm^{-1} was decreased after the drug exposure to higher humidity. The observed shifts may result from the increase of hydrogen contacts of –OH Group. The structural changes in the ritonavir sulfate exposure to higher humidity

may be associated with hydrate/pseudo polymorphic transition of the drug. These results suggested that hydrate formation took place when the drug is exposed to higher humidity. In addition, structural changes due to hydrate/pseudo polymorphic transition can easily be monitored by Raman spectroscopy.

During processing steps like crystallization and lyophilization, wet granulation and spray-drying pharmaceutical solids may come in contact with water. Further, the drug substances, which were subjected to stress conditions (different temperatures and RH environments) during storage, lead to unexpected hydration and dehydration phenomena, which affect several drug properties such as solubility, dissolution rate, stability and bioavailability [34,35]. The Raman spectra of anhydrous samples stored at different relative humidities showed evidences of the presence of hydrated samples only after $\text{RH} > 67\%$ and all the bands assigned to anhydrous ritonavir sulfate remained intact up to $65\% \text{ RH}$.

3.2.2. HPLC analysis

HPLC chromatogram illustrating hydration behavior of ritonavir sulfate under water stress condition is shown in Fig. 9. It is evident that the structure of ritonavir sulfate started changing at about $73\% \text{ RH}$. A gradual peak shift to relatively higher retention time was obtained beyond this RH value, while the drug remained stable below this humidity condition.

3.2.3. AFM analysis

The surface morphological changes of the anhydrous as well as hydrated samples of ritonavir sulfate were characterized by AFM. It is

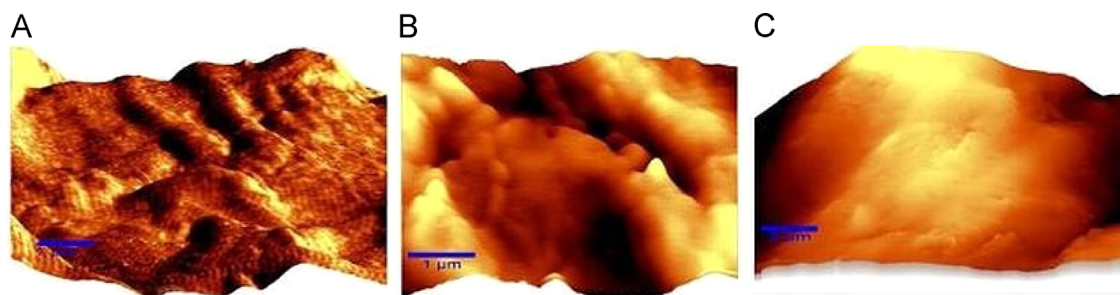


Fig. 10. AFM topographic image of ritonavir sulfate after exposing to different relative humidity environments. (A) anhydrous, (B) 28% RH and (C) 82% RH.

well known that AFM is one of effective ways for the surface analysis due to its high resolution and powerful analysis software. Fig. 10 shows AFM results before and after the drug exposure to different relative humidity environments in terms of SDR (signal of disproportionate reporting) percentage. The anhydrous form of ritonavir sulfate showed SDR 4.76538%, which was eventually reduced to SDR 1.04291% at 82% RH. Therefore, it can be concluded that morphology of the drug changed as it was exposed to different RH environments, which may be attributed to hydrate formation.

4. Conclusions

The present study assessed the feasibility of vibrational spectroscopy to evaluate the thermal stability and hydration behavior of tablet dosage form of ritonavir sulfate. From DRIFT spectroscopic investigations, it can be concluded that ritonavir sulfate started degrading around 80 °C and got completely degraded at 100 °C. All the characteristic peaks of ritonavir sulfate diminished significantly along with the emergence of a new peak at 444 cm^{-1} at 100 °C and at all temperatures beyond it. Similarly, high thermal stability of ritonavir sulfate is also confirmed through TGA/DTA investigations. Raman spectroscopic results suggested that the drug underwent structural transition as a consequence of hydration when exposed to different RH environments. The value of critical RH for ritonavir sulfate was found to be $> 67\%$. The results of hydration were confirmed by AFM analysis. In addition, HPLC results were in well agreement with DRIFT and Raman spectroscopic inferences accredited to thermal and hydration stress degradation, respectively. Further, this study was carried out to evaluate the stability of ritonavir sulfate under other stress conditions as defined by ICH guidelines.

Acknowledgments

The authors are thankful to the Director, CSIR–National Physical Laboratory, New Delhi, India, for granting the permission to publish this work.

References

- [1] S.G. Deeks, F.M. Hecht, M. Swanson, et al., HIV-RNA and CD4 cell count response to protease inhibitor therapy in an urban AIDS clinic: response to both initial and salvage therapy, *Aids* 13 (1999) F35–F43.
- [2] C.L. Dias, R.C. Rossi, E.M. Donato, et al., LC determination of ritonavir, a HIV protease inhibitor, in soft gelatin capsules, *Chromatographia* 62 (2005) 589–593.
- [3] R.N. Rao, B. Ramachandra, R.M. Vali, et al., LC–MS/MS studies of ritonavir and its forced degradation products, *J. Pharm. Biomed. Anal.* 53 (2010) 833–842.
- [4] R.S. Yekkala, D. Ashenafi, I. Mariën, et al., Evaluation of an international pharmacopoeia method for the analysis of ritonavir by liquid chromatography, *J. Pharm. Biomed. Anal.* 48 (2008) 1050–1054.
- [5] ICH Stability Testing of New Drug Substances and Products, International Conference on harmonization, IFPMA Geneva, 1993.
- [6] A. Sulebhavikar, U. Pawar, K. Mangoankar, et al., HPTLC method for simultaneous determination of lopinavir and ritonavir in capsule dosage form, *J. Chem.* 5 (2008) 706–712.
- [7] W. Gutleben, N.D. Tuan, H. Stoiber, et al., Capillary electrophoretic separation of protease inhibitors used in HIV therapy, *J. Chromatogr. A* 922 (2001) 313–320.
- [8] P.G. Wang, J.S. Wei, G. Kim, et al., Validation and application of a high performance liquid chromatography–tandem mass spectroscopy method for simultaneous quantification of lopinavir and ritonavir in human plasma using semi-automated 96-well liquid–liquid extraction, *J. Chromatogr. A* 1130 (2006) 302–307.
- [9] K.M. Rentsch, Sensitive and specific determination of eight antiretroviral agents in plasma by high performance liquid chromatography–mass spectroscopy, *J. Chromatogr. B* 788 (2003) 339–350.
- [10] E. Gangl, I. Utkin, N. Gerber, et al., Structural elucidation of metabolites of ritonavir and indinavir by LC–MS, *J. Chromatogr. A* 974 (2002) 91–101.
- [11] K. Chiranjeevi, K.P. Channabasavaraj, P. Srinivas Reddy, et al., Development and validation of spectrophotometric method for quantitative estimation of ritonavir in bulk and pharmaceutical dosage form, *Int. J. Chem. Technol. Res.* 3 (2011) 58–62.
- [12] A. Behera, S.K. Moitra, S. Si, et al., Method development, validation and stability study of ritonavir in bulk and pharmaceutical dosage form by spectrophotometric method, *Chron. Young Sci.* 2 (2011) 161–167.
- [13] J. Martin, G. Deslandes, E. Dailly, et al., A liquid chromatography–tandem mass spectrometry assay for quantification of nevirapine, indinavir, atazanavir, amprenavir, saquinavir, ritonavir, lopinavir, efavirenz, tipranavir, darunavir and maraviroc in the plasma of patients infected with HIV, *J. Chromatogr. B* 877 (2009) 3072–3082.
- [14] R. Nanda, A. Kulkarni, P. Yadav, Simultaneous spectrophotometric estimation of atazanavir sulfate and ritonavir in tablets, *Der Pharm. Chem.* 3 (2011) 84–88.
- [15] C.L. Dias, A.M. Bergold, P.E. Fröhlich, UV-derivative spectrophotometric determination of ritonavir capsules and comparison with LC method, *Anal. Lett.* 42 (2009) 1900–1910.
- [16] J.A. Droste, C.P. Verweij-Van Wissen, D.M. Burger, Simultaneous determination of the HIV drugs indinavir, amprenavir, saquinavir, ritonavir, lopinavir, nelfinavir, the nelfinavir hydroxymetabolite M8, and nevirapine in human plasma by reverse phase high performance liquid chromatography, *Ther. Drug Monit.* 25 (2003) 393–399.
- [17] G. Aymard, M. Legrand, N. Trichereau, et al., Determination of twelve antiretroviral agents in human plasma sample using reversed-phase high-performance liquid chromatography, *J. Chromatogr. B* 744 (2000) 227–240.
- [18] S. Wartewig, R.H. Neubert, Pharmaceutical applications of mid-IR and Raman spectroscopy, *Adv. Drug Deliver. Rev* 57 (2005) 1144–1170.
- [19] A. Heinz, C.J. Strachan, K.C. Gordon, et al., Analysis of solid-state transformations of pharmaceutical compounds using vibrational spectroscopy, *J. Pharm. Pharmacol.* 61 (2009) 971–988.
- [20] M.A. Bayomi, K.A. Abanumay, A.A. Al-Angary, Effect of inclusion complexation with cyclodextrins on photostability of nifedipine in solid state, *Int. J. Pharm.* 243 (2002) 107–117.
- [21] Y. Matsuda, R. Akazawa, R. Teraoka, et al., Pharmaceutical evaluation of carbamazepine modifications: comparative study for photostability of carbamazepine polymorphs by using Fourier-transformed reflection-absorption infrared spectroscopy and colorimetric measurement, *J. Pharm. Pharmacol.* 46 (1994) 162–167.
- [22] P. Singh, R. Mehrotra, A.K. Bakhshi, Stress degradation studies of nelfinavir mesylate by Fourier transform infrared spectroscopy, *J. Pharm. Biomed. Anal.* 53 (2010) 287–294.
- [23] P. Singh, L. Premkumar, R. Mehrotra, et al., Evaluation of thermal stability of indinavir sulphate using diffuse reflectance infrared spectroscopy, *J. Pharm. Biomed. Anal.* 47 (2008) 248–254.
- [24] P. Singh, G. Tyagi, R. Mehrotra, et al., Thermal stability studies of 5-fluorouracil using diffuse reflectance infrared spectroscopy, *Drug Testing Anal.* 1 (2009) 240–244.
- [25] C.J. Strachan, D. Pratiwi, K.C. Gordon, et al., Quantitative analysis of polymorphic mixtures of carbamazepine by Raman spectroscopy and principal components analysis, *J. Raman Spectrosc.* 35 (2004) 347–352.
- [26] M. Sardo, A.M. Amado, P.J. Ribeiro-Claro, Pseudopolymorphic transitions of niclosamide monitored by Raman spectroscopy, *J. Raman Spectrosc.* 39 (2008) 1915–1924.

- [27] A.M. Amado, M.M. Nolasco, P.J. Ribeiro-Claro, Probing pseudopolymorphic transitions in pharmaceutical solids using Raman spectroscopy: hydration and dehydration of theophylline, *J. Pharm. Sci.* 96 (2007) 1366–1379.
- [28] R.C. Weast, M.J. Astle, W.H. Beyer, *CRC Handbook of Chemistry and Physics*, CRC press, Boca Raton, FL, 1988.
- [29] G. Socrates, *Infrared and Raman Characteristic Group Frequencies: Tables and Charts*, John Wiley & Sons, England, 2004.
- [30] J. Machado, D. Baleanu, A.A. AL-Zahrani, et al., On similarities in infrared spectra of complex drugs, *Rom. Rep. Phys.* 66 (2014) 382–393.
- [31] N.P. Roeges, *A Guide to the Complete Interpretation of Infrared Spectra of Organic Structures*, Wiley, New York, 1974.
- [32] D.L. Pavia, G.M. Lampman, G.S. Kriz, et al., *Introduction to Spectroscopy*, Cengage Learning, USA, 2008.
- [33] F.R. Dollish, W.G. Fateley, F.F. Bentley, *Characteristic Raman Frequencies of Organic Compounds*, John Wiley & Sons, New York, 1974.
- [34] R.K. Khankari, D.J.W. Grant, *Pharmaceutical hydrates*, *Thermochim. Acta* 248 (1995) 61–79.
- [35] G. Daniele, C. Goldbronn, M. Mutz, et al., Solid state characterization of pharmaceutical hydrates, *J. Therm. Anal. Calorim.* 68 (2002) 453–465.